ELSEVIER

Biochimica et Biophysica Acta 1194 (1994) 1–11

BBA Biochimica et Biophysica Acta

Human spermatozoa glycerol permeability and activation energy determined by electron paramagnetic resonance

Junying Du [a,b], F.W. Kleinhans [a,b], Peter Mazur [c,1], John K. Critser [a,d,*]

[a] *Cryobiology Research Institute, Methodist Hospital of Indiana, 1701 N. Senate Blvd., P.O. Box 1367, Indianapolis, IN 46202, USA*
[b] *Department of Physics, Indiana University – Purdue University – Indianapolis, Indianapolis, IN 46202, USA*
[c] *Biology Division, Oak Ridge National Laboratory, Oak Ridge, TN 37831, USA*
[d] *Department of Physiology and Biophysics and OB / GYN, Indiana University, School of Medicine, Indianapolis, IN 46202, USA*

Received 7 April 1994

Abstract

The permeability of human spermatozoa to glycerol and its activation energy were determined using electron paramagnetic resonance (EPR) techniques. EPR was used to monitor the aqueous cell volume change vs. time during the glycerol permeation process using the aqueous spin label ^{15}N-tempone and the membrane impermeable broadening agent potassium trioxalatochromiate (chromium oxalate). The permeation process was completed in tens of seconds, requiring the use of a stopped-flow methodology. The glycerol permeability coefficient (P_g) was determined by fitting a simple theoretical model to the experimental data. The permeabilities of human spermatozoa in 1 molar and 2 molar glycerol at 20°C are $(10.3 \pm 0.3) \cdot 10^{-4}$ cm/min (mean ± S.D.) and $(6.0 \pm 1.4) \cdot 10^{-4}$ cm/min, respectively. The permeabilities of human spermatozoa in 2 molar glycerol at 30, 20, 10, and 0°C are $(8.3 \pm 1.3) \cdot 10^{-4}$ cm/min, $(6.0 \pm 1.4) \cdot 10^{-4}$ cm/min, $(2.1 \pm 0.4) \cdot 10^{-4}$ cm/min, and $(1.1 \pm 0.3) \cdot 10^{-4}$ cm/min, respectively. The activation energy (E_a) for glycerol permeation between 30°C and 0°C was found to be 11.6 kcal/mol.

Key words: Erythrocyte; Membrane; EPR; Glycerol permeability; Activation energy; (Human spermatozoon)

1. Introduction

There has been considerable progress in using molecular biological techniques to elucidate the nature of ion and water channels [1] in the plasma membranes of a number of cell types; however, little is known about the mechanisms and pathways for the permeation of non-electrolyte solutes. When molecular mechanisms are proposed, they have to be consistent with the phenomenological kinetics of solute permeation. In spermatozoa, there is a paucity of phenomenological information regarding such permeation kinetics, and even less information on molecular mechanisms of membrane transport.

One particular interest in the permeation kinetics of water and glycerol of sperm lies in the central importance of these parameters in determining the osmotic responses of sperm during cryopreservation. These osmotic responses can determine whether or not cells survive cooling and warming and serve as the basis for optimizing cryopreservation procedures [2–5].

A classic approach to determine solute permeabilities is to determine the time to lysis of cells placed in solutions hypertonic with respect to a permeating solute and hypotonic with respect to the non-permeating salts [6–8]. Cells placed in such solutions initially dehydrate and shrink, then re-expand as the solute permeates and water returns to maintain osmotic equilibrium with the extracellular medium. The rate of swelling is a

Abbreviations: EPR, electron paramagnetic resonance; ^{15}N-tempone, 4-oxo-2,2,6,6-tetramethyl-piperidine-1-^{15}N-1-oxyl; CrOx (potassium chromium oxalate), $K_3[Cr(C_2O_4)_3] \cdot 3H_2O$; TALP, modified Tyrode's medium with albumin, lactate and pyruvate; mOsm, milliosmolality; PBS, phosphate-buffered saline; L_p, membrane water permeability (μm/min per atm); P_g, membrane glycerol permeability (cm/min); E_a, activation energy (kcal/mol).

* Corresponding author. Fax: +1 (317) 9295347.

[1] The submitted manuscript has been authored by a contractor of the U.S. Government under contract No. DE-AC05-84OR21400. Accordingly, the U.S. Government retains a nonexclusive, royalty-free license to publish or reproduce the published form of this contribution, or allow others to do so, for U.S. Government purposes.

Elsevier Science B.V.
SSDI 0005-2736(94)00105-X

measure of the permeability of the cell to the solute. In large cells like mouse embryos, the kinetics of swelling can be directly determined by direct microscopic image analysis [9]. Optical, stopped-flow light-scattering techniques have also been used in the measurement of membrane permeabiiites; e.g., the human red cell water permeability measurements of Mlekoday et al. [10].

For mammalian sperm, microscopic methods for tracking dynamic volume changes are not currently possible because of their small size and non spherical shape. Light scattering could be used in principle; however, it is difficult to minimize artifacts from mixing transients and changes in cell shape. These artifacts are likely to be especially severe in sperm because of their highly non-spherical shape.

In our experiments, electron paramagnetic resonance (EPR) was utilized to determine cell permeability by measuring the cell aqueous volume as a function of time in a stopped-flow apparatus. The methodology involves labeling the cell suspension with a membrane-permeable aqueous spin probe (tempone), eliminating the extracellular signal with a membrane impermeant broadening agent (potassium chromium oxalate; CrOx), and tracking the intracellular signal amplitude as a function of time after exposure to glycerol. The use of a spin probe with an extracellular broadening agent to investigate intracellular water was first reported by Keith and Snipes [11] and the introduction of CrOx as an improved broadening agent was made by Berg and Nesbitt [12] and Yager *et al.* [13]. Hammerstedt et al. [14,15] pioneered the application of EPR methods to mammalian sperm and Kleinhans et al. [16] have recently reported on the specific use of tempone and CrOx with human sperm. Kinetic studies using EPR have been reported by several investigators including Vistnes and Puskin [17], Anzai et al. [18], and Moronne et al. [19].

The purpose of our experiments was to determine the value of the permeability coefficient for glycerol in 1 and 2 molar (M) solutions at room temperature and in 2 M glycerol at several temperatures using EPR. From the latter data the activation energy for the process has been calculated. To validate the EPR methodology, P_g in human red blood cells (RBC) was measured and compared to previously published values obtained by other methods.

2. Materials and methods

2.1. Chemicals

The ^{15}N-tempone (4-oxo-2,2,6,6-tetramethyl-piperidine-1-^{15}N-1-oxyl) was obtained from MSD Isotopes, Montreal, Canada. Potassium trioxalatochromiate (chromium oxalate, CrOx, $K_3[Cr(C_2O_4)_3] \cdot 3H_2O$) was synthesized according to the procedure of Bailar and Jones [20], and spectrophotometric grade glycerol was obtained from Aldrich Chemical, Milwaukee, WI.

2.2. Buffers and osmolalities

Osmolalities of the stock buffers and CrOx solutions were measured with a freezing point depression osmometer (Advanced DigiMatic Osmometer, Model 3D2) and are accurate to ± 5 milliosmolality (mOsm). Final mixture osmolalities, e.g., for the 2 molar glycerol test solution, are above the reliable range of measurement of the osmometer and were computed theoretically. This was done by (i) assuming that the buffers were pure NaCl solutions with an osmolality equal to the measured buffer osmolality, (ii) computing the water content and moles of each solute in the final mixture, (iii) adding these to find the total water and solute content of the final mixture, (iv) converting these solute concentrations back to osmolalities and (v) adding the osmolalities of each distinct constituent linearly.

The tables of Scatchard et al. [21] and the Handbook of Physics and Chemistry [22] were used for conversions between molar (M), molal (m), and osmolal (M) quantities for glycerol and NaCl. The solution properties of CrOx were measured in our lab by preparing solutions of known molarity and measuring their density (ρ) and osmolality, Table 1. The CrOx molality can be computed from the density, molarity, and molecular weight (MW = 487.4), using $m = 1000 \cdot M/(1000\ \rho - M \cdot MW)$, from the Handbook of Physics and Chemistry [22]. For the measured solution osmolalities, the osmotic coefficient of CrOx (ϕ) is computed using $\phi = M/\nu m$ where ν is four, for the stoichiometric dissociation of CrOx. The measured ϕ values are fit to a third order polynomial which then permits M to be computed for any value of m (in the range 0–250 mM CrOx) using $M = \phi \nu m$.

Red blood cells were processed in phosphate-buffered saline (PBS) with a pH of 7.4 and a mOsm of 290. The human sperm were processed in a modified Tyrode's medium, TALP, [23] with a composition per

Table 1
Solution properties of CrOx

M	m	M	ρ	ν	ϕ
0.0	0.0	0.0	0.9975	4	1.0
0.0312	0.0314	0.0927	1.012	4	0.738
0.0625	0.0633	0.1737	1.018	4	0.686
0.125	0.128	0.322	1.040	4	0.629
0.250	0.265	0.578	1.066	4	0.545

For test solutions of molarity (M), the osmolality (M) and density (ρ) were measured, and the molality (m) and osmotic coefficient (ϕ) were computed (see text), using a dissociation coefficient (ν) of 4 for CrOx.

500 ml solution of NaCl (2.77 g), KCl (118 mg), $CaCl_2 \cdot 2H_2O$ (147 mg), $MgCl_2 \cdot 6H_2O$ (51 mg), $NaHCO_3$ (1.05 g), NaH_2PO_4 (216 mg), glucose (451 mg), 60% Na lactate syrup (0.957 ml), sodium penicillin G (33 mg; 1670 units/mg), streptomycin sulfate (50 mg; 750 units/mg), BSA fraction V (2 g), pyruvic acid (18 mg), and Phenol red (5 mg) with an osmolality of 0.280 Osm.

Errors in the solution osmolalities will lead to errors in the computed P_g values. Using the modeling equations described later, it was found that a 10 mOsm error in concentration of the non-permeating salts or a 30 mOsm error in concentration of the glycerol leads to an error of $\leq 1\%$ in P_g.

2.3. Human RBC preparation

Human blood was obtained from two healthy donors by venipuncture into 8 cc vacutainer tubes with acid citrate dextrose (ACD) anticoagulant. Cells were washed three times in PBS by centrifugation at $1000 \times g$ for 5 min each, prior to use.

2.4. Human sperm preparation

Human semen samples were obtained from fifteen normal donors by masturbation after at least two days sexual abstinence. Samples were allowed to liquefy in an incubator (5% CO_2/95% air, 37°C, high humidity) for approx. 30 min; then a computer assisted semen analysis (CASA) was performed (CellSoft®, CryoResources, New York) to determine cell concentration and percent of motile sperm [24,25]. Sperm were isolated as described below in TALP buffer.

A swim-up procedure was performed by overlaying 250 μl of semen with 500 μl of TALP, incubating for approx. 1.5 h, then aspirating 400 μl of the supernatant. Since a large number of sperm were needed for the experiments, three semen samples were prepared separately by swim-up and the supernatants were pooled and held in the incubator until used, within 4 h. The original semen samples used in this experiment had motilities higher than 40% and after swim-up preparation, all motilities exceeded 80%.

2.5. EPR procedures

The samples of human sperm exposed to 1 M glycerol were prepared using 7 μl of 50 mM ^{15}N-tempone, 35 μl of 250 mM CrOx in water, 77.7 μl of water, 12.8 μl of glycerol, and 42.5 μl of packed cells in TALP (swim-up prepared sperm centrifuged at $400 \times g$ for 10 min). This solution had a total volume of 175 μl with final concentrations of 2 mM ^{15}N-tempone, 50 mM CrOx, 1 M (1.10 m) glycerol, and a final nonpermeating salt concentration of 230 mOsm due to the CrOx and TALP. The final, non-permeating solute concentration of 230 mOsm yields a greater (and therefore more easily measured) volume expansion than 290 mOsm; while being high enough to avoid cell lysis [26].

The samples of human sperm exposed to 2 M glycerol contained 7 μl of 50 mM ^{15}N-tempone, 35 μl of 250 mM CrOx in water, 74.9 μl of water, 25.6 μl of glycerol, and 32.5 μl of packed cells in TALP. This solution had a total volume 175 μl with final concentrations of 2 mM ^{15}N-tempone, 50 mM CrOx, 2 M (2.39 m) glycerol, and a final nonpermeating salt concentration of 230 mOsm due to the CrOx and TALP.

A 'background sample' was prepared for each glycerol concentration as outlined above but with buffer substituted for packed cells. All experiments were corrected for residual extracellular background by subtracting the background signal from the cell suspension signal [16–18].

Due to the rapid permeation of the glycerol through the human sperm cell membrane, a stopped-flow mixing system utilizing two pipettes was used for the sperm experiments and some of the RBC control experiments. One pipette contained the tempone, part of the CrOx, part of the water, and the packed cells in buffer. The other pipette contained the glycerol and the remainder of the CrOx and water. The osmolality of the solution in the pipette containing the cells was kept at 280–290 mOsm before injection both for the 1 M and 2 M glycerol experiments.

The permeability of human RBC to glycerol was measured using both a stopped-flow and a standard EPR protocol. The stopped-flow protocol for human RBC is the same as that for human sperm except the latter used PBS in place of TALP. In the standard protocol, the volume used was reduced to 70 μl from the stopped-flow protocol and the solutions were mixed in a 5 ml culture tube, drawn into a 50 μl micropipette (Clay Adams No. 4622, Parsippany, NJ) by capillary action, and sealed with Critoseal® (Monoject Scientific, St. Louis, MO).

Electron paramagnetic resonance measurements were made on a Varian X-Band E109 spectrometer with a rectangular cavity, temperature control (accuracy within ±0.5 C°), and an HP9825 data system with custom software for biological spin label work [27]. For the stopped-flow permeability measurements, the spectrometer is tuned to the positive peak of the low-field line and the amplitude recorded for 4 to 5 min at a sampling rate of 4 s^{-1}, yielding a time resolution of 0.25 s. The spectrometer settings were: (1) power = 20 milliwatts; (2) magnetic field ≈ 3307 gauss, centered on the low-field peak; (3) modulation amplitude = 0.5 gauss PTP; and (4) amplifier time constant = 0.128 s. The high tempone concentrations (2 mM) and high-field modulation amplitude (0.5 gauss) were chosen for optimal sensitivity and lead to some broadening of the

tempone linewidth (to 0.6 gauss). As noted later, this broadening is advantageous in the kinetics experiments.

For sample handling, a glass micropipette open at both ends was placed in the EPR cavity so that new fluid samples could be injected at the top, causing the previous sample to be ejected from the bottom. With care, to minimize the introduction of air bubbles, it is possible to change samples without retuning the microwave bridge and with only a one to two second transient.

The standard protocol used with the human RBC requires repeated 10 gauss sweeps through the low-field line, yielding a time resolution (time per sweep) of 1.5 min. The other spectrometer settings used for the standard protocol are the same as listed above for the stopped-flow protocol.

The 2 M glycerol permeability measurements were made at 30, 20, 10, and 0°C. For the 20°C measurement, the samples were equilibrated at 20°C for about 3 min, then injected into the cavity. For the other temperatures, the samples were first put into a 22°C water bath and then the temperature was increased or decreased at ~1 C°/min to the final temperature. The samples were equilibrated at the final temperature for 3 min, then transferred to the EPR cavity sample dewar which was preset to the desired temperature for each measurement.

2.6. EPR measurement of cell liquid volume

Static EPR measurements of cell water volume are relatively straight forward [15,16]. The cells are suspended in a mixture of the aqueous, membrane-permeable spin label probe, tempone, and the membrane-impermeable broadening agent, CrOx. Tempone labels all aqueous regions and the CrOx broadens (nearly to extinction) the extracellular tempone signal, leaving an intracellular tempone signal proportional to the aqueous cell volume. The EPR signal intensity is approximated by $I = W^2h$, where W and h are the peak to peak line width and height, respectively, of the low-field line [28].

The signal intensity may be converted to an actual volume of water per individual cell by determining the cell concentration in the EPR sample and by calibrating the signal intensity; but this is not necessary in these experiments. The kinetic experiments only require measurements of relative volume changes, and for this, the key requirement is that the number of cells in the sample remain constant. This specifically requires that cells not undergo lysis due to volume excursions during the course of the experiment. Noiles et al. [26] have shown that appreciable lysis of human sperm cells does not occur until the solution osmolality falls below 120 mOsm and Mazur and Miller [7] found that the critical tonicity for the osmotic hemolysis of human red cells is 140 mOsm. Both values are well below the 230 mOsm used in the current experiments.

When the cell volume changes with time, the EPR interpretation becomes more complex. As the intracellular volume changes, tempone has to flow rapidly into or out of the cell to maintain concentration equilibrium so that the intracellular tempone signal intensity accurately tracks the cell aqueous volume changes. Rapid tempone equilibration (< 1 s) has been demonstrated for human RBC [19]. It has not been demonstrated for human sperm but we assume that it is comparably fast and our results (see below) are consistent with this assumption.

The addition of glycerol to the system creates another complication. If the water/glycerol partition coefficient of tempone differs significantly from unity and if the intra- and extracellular glycerol concentrations differ significantly, then the intracellular tempone signal intensity will depend on both the intracellular fluid volume and on the glycerol concentration. For example, suppose there is glycerol outside but not inside the cell and that tempone is more soluble in glycerol than water. In this case glycerol will pull tempone out of the cell giving a deflated intracellular signal intensity and an erroneously small volume. Fortunately, in practice, the problem is not serious. We show in the Discussion that large glycerol concentration differences exist only briefly at the beginning of the experiment.

Finally, for the human sperm, the requirement of rapid data acquisition does not allow time for the complete sweep of a spectral line. The line intensity (cell volume) is approximated by the amplitude of the positive peak of the low-field line. Since the line intensity is given by $I = W^2h$, it is required that the linewidth, W, of the low-field line remain reasonably constant during the course of the experiment so that I is proportional to h. Several factors, principally changing glycerol concentration, might be expected to affect the linewidth. In practice, the high tempone concentration and field modulation amplitude, chosen for optimal signal strength, broaden the EPR line and diminish the linewidth sensitivity to changes in glycerol concentration. Also, we will demonstrate later that the intracellular glycerol concentration rapidly approaches equilibrium during these experiments.

2.7. Data analysis

Determination of the glycerol permeability coefficient (P_g). When the membrane permeable solute, glycerol, is added to an isosmotic cell suspension, the cells shrink initially because the high extracellular osmotic pressure causes exosmosis of the intracellular water. Subsequently the cell volume increases as the glycerol permeates and as water concomitantly reenters the

cells. There are a number of models to choose from for analyzing these kinds of data. Mazur et al. [6] and Mazur and Miller [7] used essentially a one parameter model for the analysis of glycerol permeability in red blood cells. They found the glycerol permeability (P_g) was sufficiently slow relative to the water permeability (L_p), in RBC that the cell volume swelling in glycerol solutions was essentially controlled by the slower P_g. In human sperm, the glycerol permeability is very high (see below) and it is more appropriate to analyze the data using two, coupled flux equations; one for the glycerol flux [6] and one for the water flux [29]. Implicit in the two parameter model is the assumption that there is no interaction between the solute and solvent flux. A third approach is to utilize the non-equilibrium thermodynamic model of Kedem and Katchalsky [30] who derived a three parameter model which includes a solute-solvent interaction characterized by the reflection coefficient (σ). This three parameter model appears very attractive and has been widely applied (e.g., [5,31,32]). However the derivation assumes dilute solutions which is not the case in these experiments using two molar glycerol. Therefore the data from these experiments were analyzed using the two parameter model. Some comparative results utilizing the three parameter, Kedem-Katchalsky (K-K) model [30] are included in the discussion.

Utilizing the two parameter model, the water flux is described by:

$$dV_w/dt = L_p ART(M^i - M^e) \quad (1)$$

and the solute flux by:

$$dN_g/dt = P_g A\left(a_g^e - a_g^i\right) \quad (2)$$

where M and a are the osmolality and solute activity of the solutions, respectively. The superscripts i, and e, refer to internal and external solutions, and the subscript g refers to glycerol. The terms V_w and N_g are the volume of water and moles of glycerol in the cell at time t, respectively, while A and T are the cell area and temperature, and R is the gas constant (see Table 2).

Expressions for the solution concentrations are given by Robinson and Stokes [36]. Because of the high glycerol concentrations used, glycerol osmolality and activity are represented by quadratic functions of molality. The osmolalities of the non-permeating solutes are adequately represented by a linear fit to the data of Scatchard et al. [21]. The total osmolalities of the external and internal solutions are assumed to equal

Table 2
Definitions of major symbols

Symbol	Description	Units	Value
L_p	water permeability	μm/min per atm	parameter
P_g	glycerol permeability	cm/min	parameter
A	surface area of cell	μm^2	120 [a] 135 [b]
V_{wo}	volume of osmotically active water in cell at time $t = 0$	μm^3	17 [c] 67 [d]
$V_w(t)$	volume of osmotically active water in cell	μm^3	variable
$V(t)$	volume of osmotic water plus glycerol in cell	μm^3	variable
$N_g(t)$	femtomoles of glycerol in cell at time t	fmol	variable
t	time in contact with glycerol	s	variable
e,i	superscripts (e = external, i = internal to cell)	–	–
g,n	subscripts (g = glycerol, n = nonpermeating salts)	–	–
M_g^e	molar concentration of external glycerol	mol/liter	1 or 2
M	osmolality	osmol/kg H_2O	–
M_{no}^i	osmolality of initial (isotonic) nonpermeating salts inside cell	osmol/kg H_2O	0.290
M_n^e	osmolality of external nonpermeating salts	osmol/kg H_2O	0.230
m	molality	mol/kg H_2O	–
a	activity	mol/kg H_2O	–
ϕ	osmotic coefficient of glycerol	–	parameter
γ	activity coefficient of glycerol	–	parameter
$\bar{v}_g$	partial molar volume of glycerol	liter/mol	0.0712

[a] Area of human sperm from Van Duijn [33].
[b] Area of human RBC from [34].
[c] Osmotically active cell water volume in isotonic human sperm from Kleinhans et al. [16] and Du et al. [35].
[d] RBC isotonic cell water from [7].

Table 3
Human RBC glycerol permeability at 20°C

Method	P_g (cm/min)	
	1 M glycerol	2 M glycerol
Normal EPR protocol	$(1.85 \pm 0.1) \cdot 10^{-4}$ [a]	$(1.65 \pm 0.1) \cdot 10^{-4}$ [a]
Stopped-flow EPR protocol	–	$(2.15 \pm 0.6) \cdot 10^{-4}$ [a]
Mazur and Miller [7] 50% hemolysis method	$2.71 \cdot 10^{-4}$	$2.33 \cdot 10^{-4}$
Mazur and Miller [7] osmotic stress method	$1.90 \cdot 10^{-4}$	$2.07 \cdot 10^{-4}$
Saari and Beck [39] 50% hemolysis method	–	$(2.04 \pm 0.3) \cdot 10^{-4}$ [b]

[a] Mean ± S.D.
[b] Mean ± S.E. (standard error of the estimate).

the sum of the osmolalities of the individual components. Then:

$$M^e = M_n^e + M_g^e = \text{fixed} \quad (3)$$

$$M^i(t) = M_n^i(t) + M_g^i(t) \quad (4)$$

$$M_n^i(t) = M_{no}^i[V_{wo}/V_w(t)] \quad (5)$$

$$M_g^j = \phi_g^j m_g^j, \quad \text{where} \quad \phi_g^j = 1 + p_o m_g^j \quad (6)$$

$$a_g^j = \gamma_g^j m_g^j, \quad \text{where} \quad \gamma_g^j = 1 + g_o m_g^j \quad (7)$$

where the subscripts 'naught', n and g, refer to initial values, non-permeating solutes, and glycerol, respectively, and j = i or e. The term m is molality, ϕ and γ are the osmotic and activity coefficients of glycerol, respectively; and the constants $p_o = 0.00975$ kg/mol and $g_o = 0.0223$ kg/mol are interpolated [6] from the data of Scatchard et al. [21].

Taking advantage of the relationship $N_g = V_w m_g^i$, Eq. (2) for dN_g/dt can be expressed as:

$$dm_g^i/dt = P_g(A/V_w)\left(a_g^e - a_g^i\right) - L_p(A/V_w)m_g^i RT(M^i - M^e) \quad (8)$$

The total volume of water and glycerol in the cell at time t is given by:

$$V(t) = V_w(t) + V_g(t) = V_w(t) \cdot \left(1 + m_g^i \bar{v}_g\right) \quad (9)$$

where $\bar{v}_g$ is the partial molar volume of glycerol.

Eqs. (1) and (8) are solved numerically using the Adaptive Runge-Kutta method as implemented in the program Diffeq® (MicroMath Scientific Software, Salt Lake City, UT). Numerical values of the constants and appropriate units are shown in Table 2.

The surface area of human spermatozoa has been computed from the measurements of Van Duijn [33] to be 120 μm^2. It is assumed constant, independent of the cell volume, because cell membranes are incapable of withstanding more than minute amounts of stretch or compression [37]. It has been argued, in the case of spherical cells such as ova, that the effective surface area increases/decreases during cell expansion/shrinkage because of folding and invagination of the cell surface [38]. We consider this unlikely for the human sperm which, because of its highly non-spherical shape, can readily change volume by re-adjusting its shape without any change in surface area. If the surface area, A, is an over (or under) estimate, the P_g value would be correspondingly lower (or higher), since P_g and A appear as a product in Eq.(2).

The isotonic water volume of human spermatozoa is 20 μm^3 [16], of which 17 μm^3 (85%) is osmotically active [35]. The water permeability, L_p, is 2.4 μm/min per atm at 22°C with an activation energy, E_a, of 2.4 kcal/mol [26]. From these values, L_p at the required temperatures is computed assuming an Arrhenius type relationship. For this high L_p value (relative to P_g), the results are insensitive to the exact value used.

To determine P_g, its value in the theoretical permeation equations was adjusted until the computed swelling curve most closely overlaid the experimental one. Differences of ±8% in P_g are readily distinguishable. When doing this, both the experimental and theoretical curve heights were scaled to the same $t = \infty$ amplitude and the time axis was shifted for best alignment.

3. Results

3.1. Human RBC permeability validation data

Results for the stopped-flow and standard EPR protocols for RBC glycerol permeability are summarized in Table 3 and yield a mean glycerol permeability at 20°C of $1.88 \cdot 10^{-4}$ cm/min.

3.2. Human sperm permeability

The data regarding the permeability of human sperm to glycerol in 1 and 2 M solutions at 20°C and in 2 M solutions at 30, 20, 10, and 0°C are summarized in

Table 4
Values of glycerol permeability, P_g, determined by EPR stopped-flow measurements in human sperm for different glycerol concentrations and temperatures

Concn. of glycerol (molar)	No. of expts.	Temp. (°C)	M_n^e (Osm)	m_g^e (molal)	P_g (10^{-4} cm/min) $\bar{x} \pm$ S.D.
1	3	20	0.23	1.10	10.3 ± 0.3
2	9	30	0.23	2.39	8.3 ± 1.3
2	8	20	0.23	2.39	6.0 ± 1.4
2	12	10	0.23	2.39	2.1 ± 0.4
2	8	0	0.23	2.39	1.1 ± 0.3

M_n^e and m_g^e are the external non-permeating buffer osmolality and external glycerol molality, respectively. Cells are abruptly transferred from 290 mOsm buffer into the buffer plus glycerol solutions indicated.

Table 4. Fig. 1 shows representative experimental and computed curves for cell (water plus glycerol) volume as a function of time when sperm cells are exposed to 2 M glycerol at 20 and 0°C. The short plateaus to the left of zero time are the equilibrated volume of intracellular water and glycerol from the previous sample. The volume increase proceeds substantially more slowly at the lower temperature.

3.3. Human sperm activation energy

Fig. 2 is an Arrhenius plot of $\ln(P_g)$ vs. $1/T$. The linear relationship obtained is consistent with Arrhenius kinetics. Thus

$$P_g(T) = P_o\, e^{-E_a/RT}$$

where P_o is constant, E_a is the activation energy for the process, R is the gas constant ($1.987 \cdot 10^{-3}$ kcal K^{-1} mol^{-1}), and T is the absolute temperature. The E_a is calculated from the slope of the Arrhenius plot (least-squares fit) as

$$E_a = -\text{slope} \cdot R$$

The resulting E_a is 11.6 kcal/mol with a coefficient of determination, r^2, of 0.970.

4. Discussion

4.1. Validation using RBC

The stopped-flow and standard kinetics protocols for P_g in red blood cells yield results which agree, within the experimental error of the measurements, and serve as a validation for the stopped-flow protocol. For human RBC, P_g has been previously measured [7,39] and those results are summarized in Table 3 for 1 and 2 M glycerol at 20°C. Our results are in good agreement with the previous data.

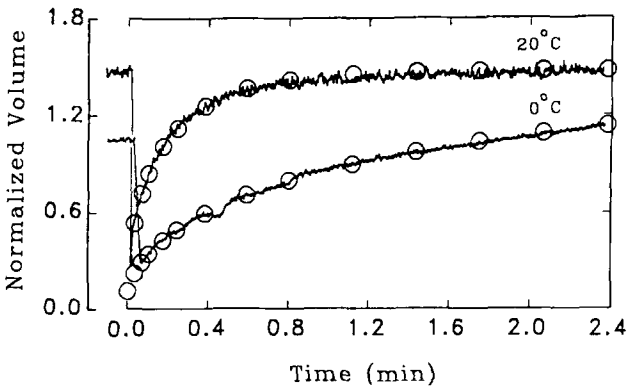

Fig. 1. Normalized volume (water plus glycerol) swell curves for human sperm at 20 and 0°C. The sperm were abruptly transferred from 290 mOsm non-permeating buffer to 2 molar glycerol in 230 mOsm buffer at $t = 0$. The solid curves show experimental EPR kinetic data obtained by monitoring the low-field peak (with extracellular background subtracted) of 2 mM ^{15}N-tempone plus 50 mM CrOx labeled cells. The superimposed computed fits (○) were obtained using $P_g = 5.5 \cdot 10^{-4}$ cm/min, $L_p = 2.33$ μm/min per atm and $P_g = 0.87 \cdot 10^{-4}$ cm/min, $L_p = 1.73$ μm/min per atm at 20 and 0°C, respectively; with negligible solute-solvent interaction assumed. The short plateau to the left of zero time is the equilibrated volume of intracellular water and glycerol from the previous sample.

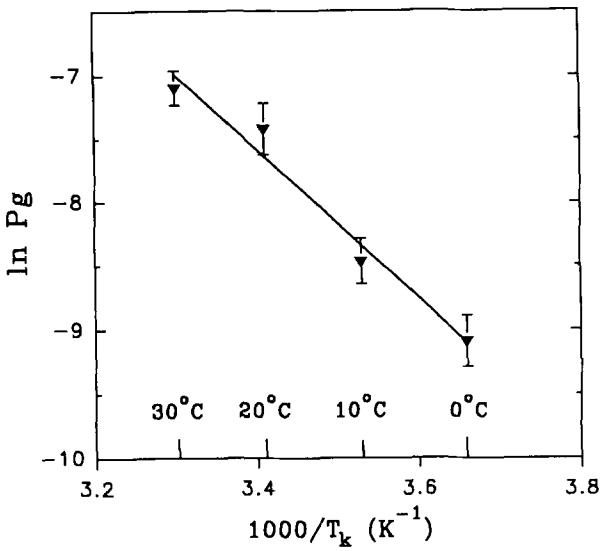

Fig. 2. Arrhenius plot of P_g for human spermatozoa in 2 molar glycerol and 230 mOsm non-permeating buffer. The computed activation energy ($E_a = -\text{slope} \cdot R$) is 11.6 kcal/mol with $r^2 = 0.970$.

4.2. P_g for human sperm

An important question in non-electrolyte permeability studies is that of whether the solute crosses the membrane via lipid bilayer diffusion or by carrier facilitated diffusion. The permeability and activation energy data of this paper are considered in this light, and compared with other investigations of membrane glycerol permeability, Table 5.

The value of P_g obtained in this study is 3–5-times higher than the very high glycerol permeability values obtained for human RBC [this study; 7,39]. In turn, P_g for human RBC is about 100-times higher than the bovine RBC [6], a difference that is believed to reflect the presence in the former of membrane protein carriers that facilitate transport of the solute (i.e., facilitated diffusion; [53]). The higher value of P_g for human sperm suggests that facilitated diffusion of glycerol may also operate in sperm. Jacobs et al. [54] showed that copper ions greatly slow glycerol permeation in the human RBC, presumably by 'poisoning' the glycerol carriers. It may have a similar effect in human sperm, although this was not tested. On the other hand, reported P_g values in egg phosphatidylcholine (PC) membranes are of the same magnitude ($2.1 \cdot 10^{-4}$ and $3.2 \cdot 10^{-4}$ cm/min at 20 and 25°C, respectively) as found in the human RBC and sperm, Table 5 [43,51].

Table 5
Selected glycerol permeability studies

Membrane	P_g (10^{-4} cm/min)	Temp. (°C)	E_a^+ (kcal/mol)	σ
Human sperm [a]	8.2	20	11.6	–
Human sperm [b]	15.	20	11.8	–
Human RBC [c]	2.5	20	7.2	–
Human RBC [d]	–	24	–	0.88
Human RBC [e]	–	–	–	0.88
Bovine RBC [f]	0.021	20	21.	–
Bovine RBC [g]	0.12	25	–	0.92
Bovine RBC [h]	–	–	–	0.99
Canine RBC [h]	–	–	–	0.97
Porcine RBC [i]	0.025	20	18.6	–
Mouse ova, unfertilized [j]	0.1	20	28.4	–
Mouse ova, fertilized [j]	0.34	20	18.7	–
Human platelet [k]	0.14	20	17.9	0.9–1.
Human platelet [l]	0.037	20	19.8	≈ 1
Human platelet [m]	2.1	37	–	–
Human granulocyte [n]	0.21	26	–	–
Dunaliella parva [o]	1.7	30	–	0.87
Nitella flexilis [p]	–	22–25	–	0.80
SR vesicles [q]	–	23	–	0.86
Egg PC liposomes [r]	–	10–35	10.1–11.9	–
+ cholesterol [r]	–	10–35	15.5	–
Egg PC vesicles [j]	2.1	20	11.6	–
Egg PC bilayer [s]	3.2	25	–	–
Egg PC liposomes [t]	–	20–40	16.2–19.3	–
+ cholesterol [t]	–	20–40	14.4–17.2	–

[+] At room temperature, a $Q_{10} = 2$ process corresponds to an E_a of 11.5 kcal/mol.
[a] EPR data, this paper. Average of 1 and 2 molar glycerol data.
[b] Gao et al. [8]. Average of 1 and 2 M data interpolated from 22°C to 20°C.
[c] Mazur and Miller [7]. Average of 1 and 2 M data.
[d] Golstein and Solomon [40].
[e] Owen and Eyring [41].
[f] Mazur et al. [6]. Average of 1 and 2 M data.
[g] Farmer and Macey [32].
[h] Owen et al. [42].
[i] Brown et al. [43]. Interpolated from 25°C to 20°C. $E_a = \delta H + RT$, Cohen [44].
[j] Jackowski et al. [9].
[k] Arnaud and Pegg [5]. Extrapolated from 21°C to 20°C.
[l] Armitage [45]. Extrapolated from 25°C to 20°C.
[m] Meyer and Verkman [46].
[n] Dooley [47].
[o] Enhuber and Gimmler [48].
[p] Steudle and Zimmermann [49].
[q] Kasai et al. [50].
[r] Cohen [44].
[s] Orbach and Finkelstein [51].
[t] Isaacson [52].

Thus lipid bilayer diffusion may be capable of yielding the large glycerol permeabilities found in this study.

The human sperm P_g activation energy of 11.6 kcal/mol is significantly lower than that found in many cell types such as bovine and porcine RBC and human platelets (17.9–21 kcal/mol), but significantly higher than that found in human RBC (7.2 kcal/mol) in which facilitated diffusion is presumed to occur (Table 5). The E_a of 11.6 kcal/mol for human sperm P_g lies within the observed range of 10 to 20 kcal/mol for model membranes (Table 5). Thus the human sperm P_g activation energy could be explained by simple bilayer diffusion. Resolution of the question of facilitated transport versus bilayer diffusion of glycerol in human sperm will require further work.

4.3. Protocol and analysis

The stopped-flow EPR protocol for determining P_g assumes that tempone rapidly equilibrates across the cell membrane. This is the case for RBC [19] but has not been previously demonstrated for human sperm. However, if tempone did not rapidly equilibrate (on a time scale of seconds or faster), its EPR signal would not accurately track the abrupt decrease in aqueous volume that occurs in the first few seconds (Fig. 1). Further, the good fit between theory and experiment near $t = 0$ implies rapid equilibration. If tempone were rate limiting, the observed initial volume excursion would be less than predicted by theory.

As previously noted, three models are available for analysis of the permeability data. The difference between our two-parameter model and the one-parameter model of Mazur et al. [6], is that the former incorporates the actual measured value of L_p whereas the latter assumes L_p to be infinite. Values of P_g for 1 and 2 M glycerol calculated by the former are 3 to 8% higher than those calculated by the one-parameter model. Thus, for human sperm, the difference between the two models is small compared with the experimental errors.

We briefly compare our two-parameter model with the Kedem-Katchalsky (K-K) formalism [30]. The difference between our two-parameter model and the K-K approach is that the former assumes no solute-solvent flux interaction while the latter incorporates this possibility through a reflection coefficient (σ). Sigma is constrained by the relationship

$$0 \le \sigma \le 1 - \omega \bar{v}_g / L_p$$

where ω is the permeability coefficient of the solute and, in the notation of this paper, $P_g = RT\omega$. In the limit of no solute-solvent flux interaction, σ is given by

$$\sigma = 1 - \omega \bar{v}_g / L_p = 1 - P_g \bar{v}_g / (RTL_p)$$

which in the case of human sperm and glycerol yields a value of $\sigma \approx 0.99$.

The actual value of σ for glycerol and human sperm is not known. For a number of other cell types, σ ranges from 0.80 to 1.0 (Table 5). However, the measurement of reflection coefficients is fraught with difficulties and some of the early measurements have been challenged, generally as being too low [41,53]. Thus the reflection coefficients in Table 5 should be viewed with

caution. If glycerol transport is primarily via bilayer diffusion, σ should be close to 0.99. For the purpose of further discussion, we consider a sigma of 0.80 to be a realistic lower limit.

As previously noted, we are concerned about the applicability of the K-K approach to non-dilute solutions. Nevertheless, to estimate the consequences of solute-solvent interactions, we have used the K-K equations to calculate P_g for a σ of 0.99 (non-interacting) and a lower limit of 0.80. In the non-interacting case, the K-K and two-parameter model give essentially identical volume swell curves and therefore, P_g values. Assuming a σ of 0.80, the K-K model yields a 20% reduction in P_g values. Thus, for realistic values of σ, the determination of P_g is only weakly model dependent. A primary objective of this ongoing work is to be able to model the osmotic response of sperm to glycerol. In this phenomenological context, the two parameter model yields a good fit to experimental data.

Human sperm P_g has also been measured by Gao et al. using a time-to-lysis method [8]. This involves measuring the time taken for 50% of the sperm to undergo lysis in solutions that contain hyperosmotic concentrations of glycerol in strongly hypotonic concentrations of non-permeating salt (40 mOsm). The 'time-to-lysis' data yield an activation energy of 11.8 kcal/mol and extrapolating these data at 22°C to a corresponding value at 20°C, yields P_g values of $16.3 \cdot 10^{-4}$ cm/min and $13.4 \cdot 1\,0^{-4}$ cm/min for 1 and 2 molar glycerol, respectively.

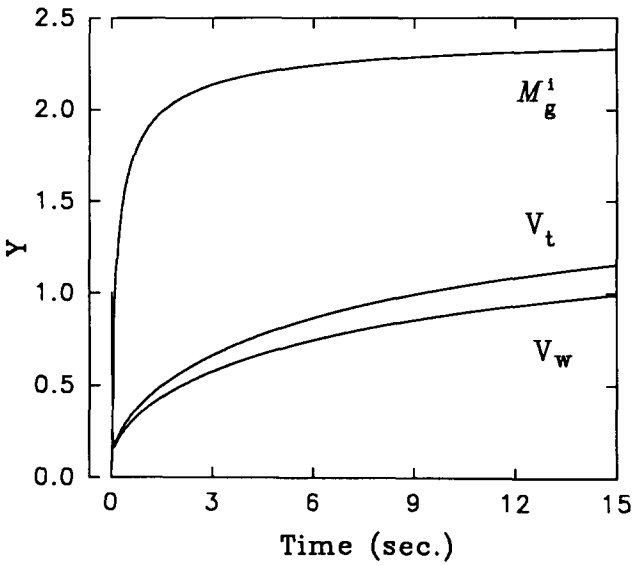

Fig. 3. Computed intracellular glycerol concentration and aqueous cell volume as a function of time at 20°C. The computation assumes isotonic sperm in 290 mOsm non-permeating buffer which are abruptly transferred at time 0 to a solution of 2 M glycerol in 230 mOsm buffer. P_g and L_p are assumed to be $6.0 \cdot 10^{-4}$ cm/min and 2.33 μm/min per atm, respectively; with negligible solute-solvent interaction. V_w and V_t are the volumes of water and water plus glycerol, respectively, normalized to the isotonic water volume at 290 mOsm. M_g^i is the osmolality of the intracellular glycerol. Note that it approaches equilibrium much more rapidly than does the aqueous volume.

There is excellent agreement between the activation energies determined by the EPR and time-to-lysis methods. However, the absolute P_g values determined by the time-to-lysis method are 1.6–2.2-times higher than the EPR derived values. Although this suggests that there are some systematic offsets between the two methods, each is internally consistent as reflected by the nearly identical E_a values. Also, the time-to-lysis data suggest a negligible concentration dependence for P_g while the EPR data suggest that P_g decreases as the glycerol concentration increases. Nevertheless, considering the major differences between these two experimental methodologies, we consider the agreement relatively good.

Among these differences are several which favor the EPR method, including: (1) the salt concentration is far above the critical tonicity and is nearer the physiological osmolality of sperm, (2) no assumptions are required concerning the independence of critical tonicity on glycerol concentration, and (3) EPR generates the entire volume 'swelling' curve and thus allows a comparison between theory and experiment over the entire curve and not just a match at the critical volume. Because of this third point, EPR may eventually be able to detect solute-solvent flux interactions. A disadvantage of the EPR experiments is that they generally are more difficult and time consuming.

Kinetic modeling. Knowledge of P_g permits one to calculate the kinetics of glycerol entry. Fig. 3 shows the modeled response (intracellular glycerol concentration, normalized cell water volume, and normalized water plus glycerol volume) of a cell exposed to 2 M glycerol (20°C) at time zero. The initial approach of glycerol *concentration* to equilibrium is much more rapid than that of the cell volume. Thus, the intracellular glycerol concentration reaches 90% of its final value within 3.4 s for sperm in 2 M glycerol (Fig. 3) and within 2.7 s in 1 M glycerol (not shown).

As noted in Materials and methods, differences (or changes) in the intra and extra-cellular glycerol concentration have the potential to create analysis problems associated with the tempone partition coefficient and changing linewidth. As shown in Fig. 3, the intracellular glycerol concentration has a rapid initial approach to equilibrium (with the outside concentration). Thus, the assumptions that underlie our EPR analysis are valid for all but the first few seconds of the volume swell curve.

Cryopreservation protocols frequently require the addition and removal of cryoprotectants such as glycerol or dimethylsulfoxide from cells, which may result in osmotic damage [4,5]. This damage can be minimized by using the P_s values to design protocols for

the stepwise addition and removal of cryoprotectant that keep osmotic volume excursions within tolerated limits. Arnaud et al. [5] illustrate the application of this approach to human platelets and glycerol; an approach which can now be applied to human sperm and glycerol.

To prevent damage from ice crystal formation during the cryopreservation of cells, cooling protocols are utilized which dehydrate the cell before intracellular freezing occurs or which vitrify the intracellular water [2,3]. In modeling these protocols in the subzero domain, the assumption is generally made that the water permeability is much higher than the cryoprotectant permeability and consequently there is a negligible flux of cryoprotectant out of the cell during cooling and freezing [3]. Our data for glycerol P_g and E_a together with the L_p and E_a data for water [26] suggest that this is a valid approximation for human sperm. The higher E_a of glycerol as compared with water means that the already large difference in membrane permeability between glycerol and water will become much greater at subzero temperatures. There is, however, need for caution. Extrapolation of the permeability parameters obtained from above 0°C measurements to below 0°C is risky at best, and measurement of subzero permeabilities and activation energies which might verify these extrapolations has proven difficult. An additional complication is the potential modifying effects of glycerol on the sperm membrane [55]. The water permeability and its activation energy of human sperm were measured in the absence of glycerol [26], however a number of studies of various cells [3,56] report a reduction of 2 or more in L_p in the presence of glycerol. Consequently these glycerol permeability studies and the previous water permeability studies in human sperm are only the first step to developing a comprehensive understanding of the permeability properties of human sperm.

Summary. Electron paramagnetic resonance has been successfully used to measure the glycerol permeability of human sperm. The value obtained is insensitive to the analysis model used and is perhaps the highest reported for any mammalian cells studied to date. Further work will be required to establish the relative importance of bilayer diffusion and facilitated transport to glycerol permeability. The EPR technique provides a useful method of measuring permeability for cell types which are small in size and/or of irregular shape.

Acknowledgments

This work was supported by Methodist Hospital Inc. of Indiana, grants from the NIH (RO1 HD-25949 and KO4-HD00980), and the Office of Health and Environmental Research, U.S. Dept. of Energy under contract DE-AC05-840R21400 with Martin-Marietta Energy. We thank Yihong Pei for assistance in the experiments and Katherine Vernon for assistance with the preparation of the manuscript.

References

[1] Verkman, A.S. (1992) Annu. Rev. Physiol. 54, 97–108.
[2] Mazur, P. (1984) Am. J. Physiol. 247, C125–C142.
[3] Mazur, P. (1990) Cell Biophys. 17, 53–92.
[4] Gao, D.Y., Ashworth, E., Watson, P.F., Kleinhans, F.W., Mazur, P. and Critser, J.K. (1993) Biol. Reprod. 49, 112–123.
[5] Arnaud, F.G. and Pegg, D.E. (1990) Cryobiology 27, 107–118.
[6] Mazur, P., Leibo, S.P. and Miller, R.H. (1974) J. Membr. Biol. 15, 107–136.
[7] Mazur, P. and Miller, R.H. (1976) Cryobiology 13, 507–522.
[8] Gao, D.Y., Mazur, P., Kleinhans, F.W., Watson, P.F., Noiles, E.E. and Critser, J.K. (1992) Cryobiology 29, 657–667.
[9] Jackowski, S., Leibo, S.P. and Mazur, P. (1980) J. Exp. Zool. 212, 329–341.
[10] Mlekoday, H.J., Moore, R. and Levitt, D.G. (1983) J. Gen. Physiol. 81, 213–220.
[11] Keith, A.D. and Snipes, W. (1974) Science 183, 666–668.
[12] Berg, S.P. and Nesbitt, D.M. (1979) Biochim. Biophys. Acta 548, 608–615.
[13] Yager, T.D., Eaton, G.R. and Eaton, S.S. (1979) Inorg. Chem. 18, 725–727.
[14] Hammerstedt, R.H., Amann, R.P., Rucinsky, T., Morse, P.D., II, Lepock, J., Snipes, W. and Keith, A.D. (1976) Biol. Reprod. 14, 381–397.
[15] Hammerstedt, R.H., Keith, A.D., Snipes, W., Amann, R.P., Arruda, D. and Griel, L.C., Jr. (1978) Biol. Reprod. 18, 686–696.
[16] Kleinhans, F.W., Travis, V.S., Du, J., Villines, P.M., Colvin, K.E. and Critser, J.K. (1992) J. Androl. 13, 498–506.
[17] Vistnes, A.I. and Puskin, J.S. (1981) Biochim. Biophys. Acta 644, 244–250.
[18] Anzai, K., Higashi, K.I. and Kirino, Y. (1988) Biochim. Biophys. Acta 937, 73–80.
[19] Moronne, M.M., Mehlhorn, R.J., Miller, M.P., Ackerson, L.C. and Macey, R.I. (1990) J. Membr. Biol. 115, 31–40.
[20] Bailar, J.C., Jr. and Jones, E.M. (1939) Inorg. Synth. 1, 35–38.
[21] Scatchard, G., Hamer, W.J. and Wood, S.E. (1938) J. Am. Chem. Soc. 60, 3061–3070.
[22] Weast, R.E. (ed.) (1970–71) in CRC Handbook of Chemistry and Physics, 51st Edn., pp. D-110, D181–D226, CRC Press, Cleveland.
[23] Bavister, B.D., Leibfried, M.L. and Lieberman, G. (1983) Biol. Reprod. 28, 235–247.
[24] Jequier, A. and Crich, J. (1986) in Semen Analysis: A Practical Guide, pp. 143–149, Blackwell Scientific Publications, Boston.
[25] Critser, J.K., Colvin, K.E. and Critser, E.S. (1988) J. Androl. 9 (Suppl.), P45.
[26] Noiles, E.E., Mazur, P., Watson, P.F., Kleinhans, F.W. and Critser, J.K. (1993) Biol. Reprod. 48, 99–109.
[27] Kleinhans, F.W. (1985) J. Magn. Reson. 65, 146–148.
[28] Wertz, J.E. and Bolton, J.R. (1972) in Electron Spin Resonance: Elementary Theory and Practical Applications, p. 34, McGraw-Hill, New York.
[29] Dick, D.A.T. (1966) in Cell Water, pp. 83–120, Butterworth, Washington, D.C.
[30] Kedem, O. and Katchalsky, A. (1958) Biochim. Biophys. Acta 27, 229–246.

[31] Levitt, D.G. and Mlekoday, H.J. (1983) J. Gen. Physiol. 81,239–253.
[32] Farmer, R.E.L. and Macey, R.I. (1972) Biochim. Biophys. Acta 255, 502–516.
[33] Van Duijn, C., Jr. (1957) J. Roy. Microsc. Soc. 77, 12–27.
[34] Evans, E. and Fung, Y.C. (1972) Microvasc. Res. 4, 335–347.
[35] Du, J., Kleinhans, F.W., Mazur, P. and Critser, J.K. (1993) Cryo-Letters 14, 285–294.
[36] Robinson, R.A. and Stokes, R.H. (1959) Electrolyte Solutions, Butterworths, London.
[37] Canham, P.B. (1970) J. Cell. Physiol. 74, 203–212.
[38] Shabana, M. and McGrath, J.J. (1988) Cryobiology 25, 338–354.
[39] Saari, J.T. and Beck, J.S. (1975) J. Membr. Biol. 23, 213–226.
[40] Goldstein, D.A. and Solomon, A.K. (1960) J. Gen. Physiol. 44, 1–17.
[41] Owen, J.D. and Eyring, E.M. (1975) J. Gen. Physiol. 66, 251–265.
[42] Owen, J.D., Steggall, M. and Eyring, E.M. (1976) J. Membr. Biol. 26, 287–299.
[43] Brown, F.F., Sussman, I., Avron, M. and Degani, H. (1982) Biochim. Biophys. Acta 690, 165–173.
[44] Cohen, B.E. (1975) J. Membr. Biol. 20, 205–234.
[45] Armitage, W.J. (1986) J. Cell. Physiol. 128, 121–126.
[46] Meyer, M.M. and Verkman, A.S. (1986) Am. J. Physiol 251, C549-C557.
[47] Dooley, D.C. (1982) Exp. Hematol. 10, 413–422.
[48] Enhuber, G. and Gimmler, H. (1980) J. Phycol. 16, 524–532.
[49] Steudle, E. and Zimmermann, U. (1974) Biochim. Biophys. Acta 332, 399–412.
[50] Kasai, M., Kanemasa, T. and Fukumoto, S. (1979) J. Membr. Biol. 51, 311–324.
[51] Orbach, E. and Finkelstein, A. (1980) J. Gen. Physiol. 75, 427–436.
[52] Isaacson, Y., Riehl, T.E. and Stenson, W.F. (1989) Biochim. Biophys. Acta 986, 295–300.
[53] Stein, W.D. (1986) in Transport and Diffusion Across Cell Membranes, pp. 231–361, Academic Press, New York.
[54] Jacobs, M.H., Glassman, H.N. and Parpart, A.K. (1935) J. Cell. Comp. Physiol. 7, 197–225.
[55] Hammerstedt, R.H. and Graham, J.K. (1992) Cryobiology 29, 26–38.
[56] Papanek, T.H. (1978), PhD Thesis, Massachusetts Institute of Technology, Cambridge, MA.